Site-Directed Disulfide Mapping of Residues Contributing to the Ca^{2+} and K^+ Binding Pocket of the NCKX2 Na^+/Ca^{2+}-K^+ Exchanger†

Tashi G. Kinjo,‡ KyeongJin Kang,‡ Robert T. Szerencsei, Robert J. Winkfein, and Paul P. M. Schnetkamp*

Hotchkiss Brain Institute, Department of Physiology and Biophysics, Faculty of Medicine, University of Calgary, 3330 Hospital Drive, Calgary, Alberta, T2N 4N1 Canada

Received February 9, 2005; Revised Manuscript Received April 5, 2005

ABSTRACT: The Na^+/Ca^{2+}-K^+ exchanger (NCKX) gene products are polytopic membrane proteins that utilize the existing cellular Na^+ and K^+ gradients to extrude cytoplasmic Ca^{2+}. NCKX proteins are made up of two clusters of hydrophobic segments, both thought to consist of five putative membrane-spanning α-helices, and separated by a large cytoplasmic loop. The two most conserved regions within the NCKX sequence are known as the α1 and α2 repeats, and are found within the first and second set of transmembrane domains, respectively. The α repeats have previously been shown to contain residues critical for transport function. Here we used site-directed disulfide mapping to report that the α repeats are found in close proximity in three-dimensional space, bringing together key functional NCKX residues, e.g., the two critical acidic residues, Glu^{188} and Asp^{548}. Glu188Cys in the α1 repeat could form a disulfide cross-link with Asp548Cys in the α2 repeat. Surprisingly, cysteine substitutions of Ser^{185} in the α1 repeat could form disulfide cross-links with cysteine substitutions of three residues in the α2 repeat (Ser^{545}, Asp^{548}, and Ser^{552}), thought to cover close to two full turns of an α helix, implying an area of increased flexibility. Using the same method, Asp^{575}, a residue critical for the K^+ dependence of NCKX, was shown to be in the proximity of Ser^{185} and Glu^{188}, consistent with its role in enabling K^+ to bind to a single Ca^{2+} and K^+ binding pocket.

The SLC24 gene family of K^+-dependent Na^+/Ca^{2+} exchangers (NCKXs)[1] consists of six distinct genes whose transcripts are found in a wide variety of tissues (*1*, *2*); several NCKX-related cDNAs have also been cloned from invertebrates on the basis of homology within hydrophobic segments of the NCKX sequence (*3*−*6*). With the possible exception of NCKX6 (*2*, *7*), all these NCKX cDNAs have been shown to encode proteins carrying out K^+-dependent Na^+/Ca^{2+} exchange transport when expressed in heterologous cell systems. NCKX1 and NCKX2 are the best studied NCKX proteins and have been shown to transport K^+ and operate at a $4Na^+$:$1Ca^{2+}$ + $1K^+$ stoichiometry (*8*−*10*). Detailed "in situ" characterization of NCKX has been limited so far to NCKX1 found in the outer segments of retinal rod photoreceptors (reviewed in refs *11*−*13*). In rod outer segments, NCKX1 is associated with the heteromultimeric cGMP-gated channel (*14*, *15*), and when expressed in cell lines, both NCKX1 and NCKX2 associate with the CNGA subunits of both the rod and cone cGMP-gated channels (*16*). As a significant fraction of the inward current through both rod and cone cGMP-gated channels is carried by Ca^{2+} (*17*, *18*), the physiological role of NCKX in vertebrate photoreceptors is removal of this Ca^{2+}.

Hydrophobicity analysis shows that all NCKX proteins contain 11 distinct hydrophobic segments (H1−H11), each of which contains some sequence that is similar to the corresponding hydrophobic segment in each of all other NCKX proteins (*6*). With the exception of the two *Drosophila* NCKXs, all other NCKX sequences contain an additional hydrophobic segment at the N-terminus, predicted to be either a cleavable signal peptide or a noncleaved signal anchor. The signal peptide of NCKX1 and NCKX2 has been shown to undergo delayed cleavage, essential for plasma membrane targeting (*19*). In addition to the hydrophobic segments, NCKX sequences contain two large hydrophilic loops that contain no sequence elements conserved among all NCKX isoforms. One large N-terminal hydrophilic loop is located in the extracellular space following signal peptide cleavage; the second hydrophilic loop in the middle of the NCKX sequence is located in the cytosol and separates two clusters of five and six hydrophobic segments. Both large hydrophilic loops can be deleted from the NCKX1 protein without any major effects on transport function or on the

† This work was supported by an operating grant from the Canadian Institutes for Health Research to P.P.M.S. P.P.M.S. is a scientist of the Alberta Heritage Foundation for Medical Research. K.J.K. is recipient of a studentship from the Foundation Fighting Blindness Canada. T.G.K. is recipient of a studentship from the Alberta Heritage Foundation for Medical Research.

* To whom correspondence should be addressed. Phone: (403) 220-5448. Fax: (403) 283-8731. E-mail: pschnetk@ucalgary.ca.

‡ These authors contributed equally to this work.

[1] Abbreviations: NCKX, Na^+/Ca^{2+}-K^+ exchanger; NCX, Na^+/Ca^{2+} exchanger; Cys-less, cysteine-free; K_d, dissociation constant; DMEM, Dulbecco's modified Eagle's medium; DTT, dithiothreitol; MW, molecular weight; IP, immunoprecipitation; IB, immunoblot; EDTA, ethylenediaminetetraacetic acid; DOC, deoxycholate; TBS, Tris-buffered saline; FBS, fetal bovine serum; TBST, Tris-buffered saline with 0.05% Tween; PBS, phosphate-buffered saline; HRP, horseradish peroxidase; DMF, dimethylformamide; PAGE, polyacrylamide gel electrophoresis; NEM, *N*-ethylmaleimide; MTSET, [2-(trimethylammonium)ethyl]-methanethiosulfonate bromide; CFTR, cystic fibrosis transmembrane conductance regulator; hERG, human ether-a-go-go-related gene; Tris, tris(hydroxymethyl)aminomethane.

10.1021/bi0502442 CCC: $30.25
Published on Web 05/07/2005

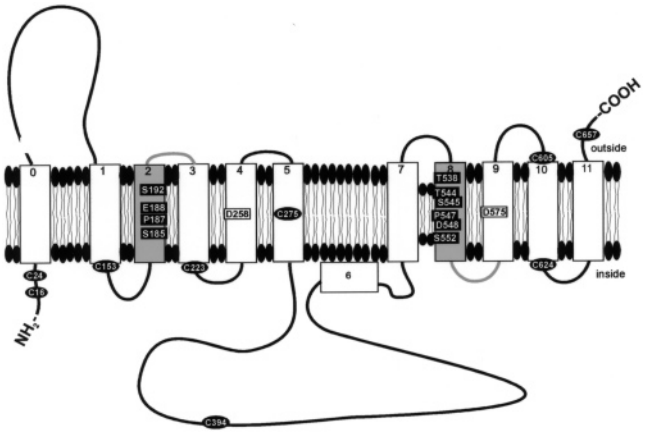

FIGURE 1: Location of endogenous cysteine residues and sites of insertion of cysteine into the Cys-less NCKX2 Na^+/Ca^{2+}-K^+ exchanger. The NCKX2 protein contains 11 hydrophobic segments (1−11) in addition to the cleavable signal peptide (0). Endogenous cysteine residues (black ovals) were replaced with serine residues to yield the Cys-less NCKX2 (*22*). The gray areas centered on helices 2 and 8 represent the α1 and α2 repeats, respectively. Double cysteine insertions into the Cys-less background were made by replacing one residue in the α1 repeat and one residue in the α2 repeat (represented by black rectangles). In addition, residues D258 in H4 and D575 in H9 were analyzed (white rectangles).

cation dependencies of Na^+/Ca^{2+}-K^+ exchange transport (*3*, *9*). Little is known about the spatial arrangement of the 11 hydrophobic segments in NCKX. Mapping of inserted glycosylation sites combined with mapping of inserted cysteine residues in NCKX2 resulted in the topology illustrated in Figure 1 (*20*), consistent with an extracellular localization of the C-terminus as reported by antibody binding to an inserted epitope at this position (*21*). In two recent studies, we reported that several residues in putative membrane-spanning helices H2, H4, H8, and H9 contribute to a single Ca^{2+} and K^+ binding pocket based on the effect of individual substitution of several of these residues on the Ca^{2+} and K^+ concentration dependencies of reverse Na^+/Ca^{2+} exchange (the location of these residues is shown in Figure 1) (*22*, *23*). This would suggest that these helices come together in the native NCKX2 structure, although they are separated in the linear sequence by ∼350 residues. Here, site-directed disulfide mapping was used to test for the proximity of these residues in helices H2 and H4 to those in helices H8 and H9. We previously generated a functional mutant NCKX2 (Cys-less), in which all nine endogenous cysteine residues (Figure 1 illustrates the position of these cysteine residues) were replaced with serine residues (*24*). Using copper-bound phenanthroline to generate intramolecular disulfide linkages between pairs of inserted cysteine residues in the Cys-less background, we demonstrate here that several residues in helix H2 are in the proximity of residues in helices H8 and to D575 in H9. The residues identified here are conserved in the NCKX1−5 isoforms, and most are among the few residues conserved between members of the NCKX gene family and members of the SLC8 gene family of Na^+/Ca^{2+} exchangers (NCX). Recently, D575 in helix H9 was shown to be critical for the K^+ dependence of NCKX2 (*23*); D575 is conserved among the NCKX1−5 isoforms, but not found in NCKX6 or in the three NCX isoforms.

EXPERIMENTAL PROCEDURES

Mutagenesis. The cysteine-free or Cys-less human NCKX2 was made as described elsewhere by replacing the codons for all nine endogenous cysteine residues with codons for serine (*24*). The residue numbering used in this and our previous studies is that of the wild-type (WT) full-length human NCKX2 (*25*). Pairs of cysteine codons were inserted at various positions into this Cys-less background as described previously (*26*). Briefly, the pEIA Cys-less NCKX2 clone was partially digested with XbaI, blunted, and religated to remove a 3′ polylinker XbaI site. The internal NCKX2 XbaI and XhoI sites were then used to clone cysteine mutants into the 5′ region of the molecule. Two internal 3′ BsrGI sites were then used to clone cysteine mutants into the second half of the molecule. All mutants made using the BsrGI sites were PCR screened for the proper insert number and orientation. All PCR-generated fragments were sequenced after insertion to ensure no unwanted mutations were generated through PCR errors. Plasmid DNAs were prepared using the EndoFree Plasmid Maxi Kit system from Qiagen (Mississauga, ON).

Copper−Phenanthroline Treatment. We used an insect cell line (High Five cells) for transient transfection with the various double cysteine insertion NCKX2 mutants as described previously (*3*). Two days after transfection, High Five cells were washed with a medium containing 150 mM KCl, 80 mM sucrose, and 20 mM Hepes (adjusted to pH 7.4 with arginine) and resuspended in 150 mM KCl and 20 mM Mops (adjusted to pH 7.4 with arginine). In some experiments, the human embryonic kidney cell line (HEK293) was used as described previously (*19*). Two days after transfection, HEK293 cells were washed twice on the plate with PBS [140 mM NaCl, 2.7 mM KCl, 10 mM Na_2HPO_4, and 1.8 mM KH_2PO_4 (pH 7.4)], lifted from the plate in PBS, and collected by centrifugation (3 min at 300*g*). The pellet was resuspended in PBS to a final protein concentration of 5 mg/mL. The HEK293 cell or High Five cell suspension (1−2 mg of protein/mL) in the media described above was incubated with 2 mM phenanthroline and 1 mM $CuSO_4$ for 10 or 60 min at room temperature as indicated in the text. The reaction was terminated by addition of 5 mM EDTA. The final pellet was resuspended in 150 mL of lysis buffer containing 1% Triton X-100, 0.5% DOC, 140 mM NaCl, 25 mM Tris (pH 7.5), 10 mM EDTA, and one protease inhibitor tablet per 10 mL (Complete, Mini, Roche), incubated on ice for 20 min, and spun down at 20000*g*. An aliquot of the supernatant containing 20 μg of total protein was separated on an 8% Laemmli gel, transferred to a nitrocellulose membrane, and probed overnight at 4 °C with the monoclonal c-myc antibody (NEB, Pickering, ON) (1:2000 dilution in TBST with 1% skim milk added) using standard procedures (*3*). The resulting films (Kodak Biomax Light, Eastman Kodak Co., Rochester, NY) were scanned and analyzed with SigmaGel 1.0. In earlier experiments, 1 mM DTT was added to the sample buffer to reverse disulfide bond formation. For the double cysteine insertion mutants expressed in HEK293 cells, some intramolecular cross-linking could occur in the lysis buffer without copper−phenanthroline being present. Therefore, in later experiments, cells were incubated with 5 mM *N*-ethylmaleimide (NEM) for 10 min to block all remaining free sulfhydryl groups prior to addition of lysis

buffer. In control experiments, cells were treated with NEM first, and then treated with copper−phenanthroline. Most of the NEM was removed by a single sedimentation step (3 min at 300*g*) and resuspension of the cell pellet in NEM-free medium.

Surface Biotinylation of Wild-Type NCKX2 and NCKX2 Mutants. Cells were transfected with the various cysteine insertion mutant NCKX2 cDNAs as described previously (*24*). Biotinylation was carried out in PBS medium with 80 mM added sucrose and 1 mM EZ-Link Sulfo-NHS-LC-Biotin (Pierce, Rockford, IL) for 7 min. The reaction was terminated by incubation for 20 min with 250 mM Tris-HCl (pH 7.5). In some experiments, cells were subsequently treated with copper−phenanthroline and NEM as described above. When no additional copper−phenanthroline treatment was carried out, cells were washed two times in the PBS medium described above, incubated for 20 min with ice-cold lysis buffer, and sedimented (5 min at 20000*g*), and the supernatant was used. Protein concentrations were determined with the Bradford reagent. Samples containing 1 mg of total protein were incubated for 2 h on ice with 1 μL of monoclonal Myc antibody (NEB Biolabs). Subsequently, these samples were mixed with protein A/G Plus−agarose beads (Santa Cruz Biotechnology). The beads were incubated overnight at 4 °C, and then washed three times with PBST containing 10 mM Na_2HPO_4, 1.8 mM KH_2PO_4, 140 mM NaCl, 2.7 mM KCl, and 0.1% Tween 20 (pH 7.4). After addition of the sample buffer, the beads were heated for 2 min at 95 °C and aliquots were subjected to gel electrophoresis in an 8% Laemmli gel, transferred to nitrocellulose paper, and probed with 0.4 μg/mL avidin−HRP (Biolynx Inc., Brockville, ON).

RESULTS

Formation of a Disulfide Bond between Inserted Cysteine Residues in Probing Residue Proximity. In two recent studies (*22*, *23*), we identified 10 residues in the human NCKX2 protein that were important for NCKX transport function (E188, P187, and S185 in H2; D258 in H4; T544, S545, P547, D548, and S552 in H8; and D575 in H9) (Figure 1). Individual substitution of several of these residues, in particular, E188 and D548, resulted in mutant NCKX2 proteins that displayed shifts in both the K^+ and Ca^{2+} concentration dependencies of reverse Na^+/Ca^{2+}-K^+ exchange transport (Ca^{2+} influx), suggesting these residues contribute to lining the NCKX cation binding pocket. Eight of the 10 residues described above are located in two membrane-spanning helices (H2 and H8), part of the so-called α1 and α2 repeats and separated by ~350 residues as illustrated in Figure 1. Residue D575 in H9 was shown to be critical for the K^+ dependence of NCKX2 and was suggested to facilitate binding of K^+ to a common Ca^{2+} and K^+ binding site (*23*). If the above residues combine to line the cation binding pocket, they should be in close apposition in the native NCKX2 conformation. We previously generated a functional Cys-less NCKX2 mutant in which all endogenous cysteine residues were replaced with serine residues, and which exhibited wild-type protein expression and ~50% of wild-type NCKX2 transport activity (*24*). To address the proximity of residues thought to be important for cation binding, we carried out site-directed disulfide mapping. We selected S185 and E188 as two key residues in H2 of the α1 repeat and S545, D548, S552 (all three in H8), and D575 (in H9) as critical residues in the α2 repeat. Pairs of cysteine residues were introduced, one cysteine replacing either S185 or E188 in helix H2 and the other cysteine replacing either a single residue in helix H8 or D575 in H9. The double cysteine insertion mutants were expressed in the insect High Five cell system, previously reported to yield very consistent expression of both NCKX protein and NCKX function for a large range of NCKX clones and NCKX2 mutants (*3*, *19*, *26*).

Signal Peptide Cleavage and Expression Levels of the Double Cysteine Insertion Mutants. The residues selected for this disulfide mapping study are critical for NCKX transport function, and as a result, most of the double cysteine insertion mutants exhibited very little or no NCKX transport function when analyzed in either High Five or HEK cells (not illustrated). Therefore, these nonfunctional NCKX2 mutants could conceivably be incorrectly folded proteins, retained within the cell, and not representing the wild-type NCKX2 structure. Moreover, overexpression of plasma membrane proteins in cell lines often results in a large amount of expressed protein retained in intracellular membranes, and this may present immature or incorrectly folded protein as well. Heterologous expression of NCKX2 in cell lines invariably yielded a two-band pattern of NCKX2 when analyzed on SDS−PAGE. We have previously shown that the lower band represents the NCKX2 protein that has undergone delayed cleavage of an N-terminal signal peptide and only the NCKX2 protein represented by the lower band is present in the plasma membrane, while the NCKX2 protein represented by the noncleaved upper band is retained within the cell (*19*). Hence, the two-band pattern serves as a convenient indicator of NCKX2 protein maturation and plasma membrane targeting. In all (>120) mutant NCKX2 constructs examined by us so far, signal peptide cleavage was invariably associated with plasma membrane delivery (*19*, *22*, *26*) (see also Figure 7). All the double cysteine insertion mutants used in this study exhibited the two-band pattern when analyzed on SDS−PAGE, suggesting that at least a fraction of the mutant NCKX2 protein had undergone proper signal peptide cleavage and was correctly targeted to the plasma membrane. To quantify peptide cleavage and expression levels, all Western blots of the double cysteine insertion mutant NCKX2 were scanned and the ratio of lower (cleaved) to upper (noncleaved) band was obtained (Figure 2). The results show that signal peptide cleavage for the above-mentioned double cysteine insertion mutants was quite similar when compared to that of the functionally active Cys-less NCKX2. The double mutants with the S192 and D258 residues (see below) were also analyzed, and in this case, the extent of signal peptide cleavage was somewhat reduced, in particular, for the D258C/D575C mutant. Average protein expression levels of the lower band representing cleaved NCKX2 were within 25% of that of the Cys-less NCKX2 except that expression levels for the D258C/D575C mutant NCKX2 were only 15% of that of the Cys-less NCKX2 (data not illustrated). Typical examples of the two-band pattern exhibited by the various NCKX2 mutants can be found in Figures 3A, 5A, and 6A.

Disulfide Bond Formation by Copper−Phenanthroline: S185C and E188C in Helix H2 Can Each Form Intramolecular Cross-Links with Several Residues in Helix H8

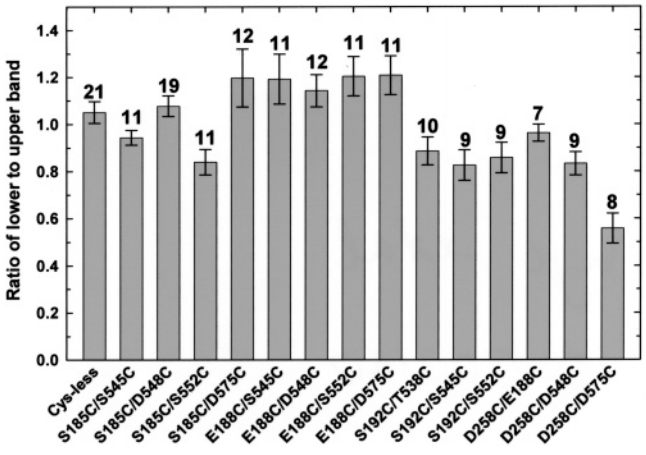

FIGURE 2: Signal peptide cleavage in the double cysteine insertion mutant NCKX2 proteins. The Cys-less NCKX2 protein and the indicated double cysteine insertion mutants in the Cys-less background were expressed in High Five cells. Protein samples (20 μg of protein/lane) were separated on SDS−PAGE, transferred, and analyzed by Western blotting with the monoclonal Myc antibody. The blots were scanned, and with the use of SigmalGel 1.0, the ratio of the lower band (representing cleaved mutant NCKX2) to the upper band (representing noncleaved mutant NCKX2) was determined. Average values (±standard error of the mean) are shown for the indicated number of experiments.

and with D575 in Helix H9. Disulfide mapping was carried out by treatment with copper−phenanthroline as described in Experimental Procedures. Figure 3A illustrates the results for the double cysteine insertion mutants when either S185C in H2 or E188C in H2 is paired with each of three different residues in H8 or with D575C in H9. Disulfide bond formation was assessed as a molecular weight (MW) shift on SDS−PAGE. All samples were separated on SDS−PAGE under nonreducing conditions and analyzed for apparent MW shifts on the basis of the premise that an intramolecular disulfide bond will prevent complete unfolding of the NCKX2 protein under denaturing conditions in the presence of SDS and this is likely to affect protein mobility. As expected, copper−phenanthroline treatment did not induce a shift in mobility on SDS−PAGE for the Cys-less NCKX2. However, significant shifts in mobility were observed for all the S185C and E188C double mutants tested here, demonstrating that an intramolecular disulfide bond had formed which prevented complete unfolding of the mutant NCKX2 protein in the SDS sample buffer and resulted in the increased mobility observed on SDS−PAGE. When the cross-linked samples were treated with 1 mM DTT prior to SDS−PAGE, all mutants exhibited the two-band pattern observed for the Cys-less NCKX2, indicating that the disulfide bonds could be readily reduced (Figure 3A). When free sulfhydryl groups were alkylated with NEM prior to copper−phenanthroline treatment, no intramolecular cross-links were observed, while addition of NEM after copper−phenanthroline treatment did not reverse intramolecular cross-linking (data not illustrated).

Copper−phenanthroline treatment of the three double cysteine mutants with residues in H8 resulted in a four-band pattern for both S185C and E188C. This suggests that NCKX2 mutant proteins could readily form intramolecular disulfide cross-links irrespective of signal peptide cleavage. This result is not unexpected since copper−phenanthroline is a membrane permeable reagent and should be able to have

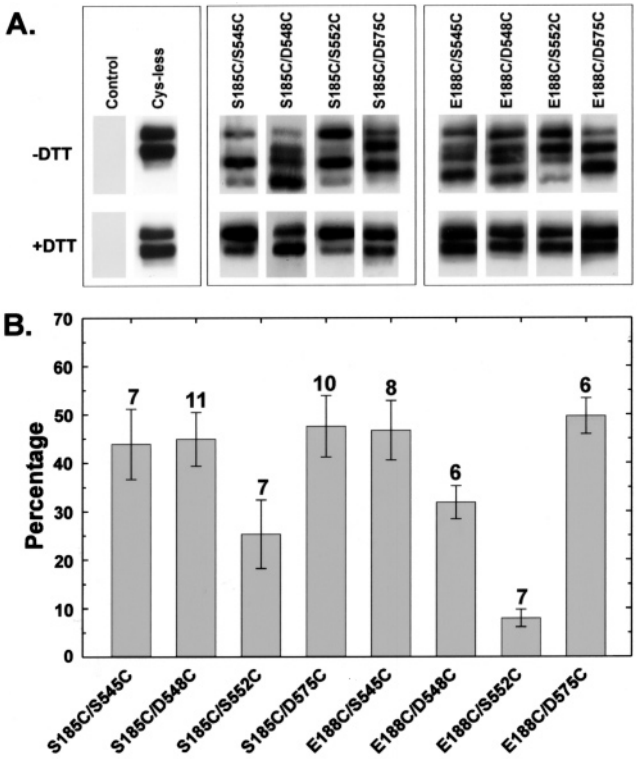

FIGURE 3: Intramolecular disulfide bond formation as an indicator of residue proximity. (A) The Cys-less NCKX2 and the indicated double cysteine insertion mutants in the Cys-less background were expressed in High Five cells and treated with copper−phenanthroline (as described in Experimental Procedures). Control represents mock-transfected cells. Protein was extracted in lysis buffer, and samples (20 μg of protein/lane) were separated by SDS−PAGE under nonreducing conditions (top panels labeled −DTT); samples to which 1 mM DTT was added are illustrated in the bottom panels (labeled +DTT). The Myc-tagged NCKX2 mutants were visualized with the monoclonal Myc antibody. Shifts in mobility compared to the Cys-less NCKX2 indicate intramolecular disulfide bond formation. (B) Western blots of experiments such as the one illustrated in panel A were scanned and analyzed with the use of SigmaGel 1.0. The area representing the lowest band was expressed as the percentage of the total NCKX2 protein present (total area representing all bands). Average values (±standard error of the mean) are shown for the various NCKX2 mutants with the number of independent experiments indicated at the top of the bars.

access to uncleaved NCKX2 that did not reach the plasma membrane. In some gels, the two middle bands merged into a single band, and in the case of the S185C/D575C NCKX2 and E188C/D575C NCKX2 double mutants, a four-band pattern was generally not resolved. In this case, we believe the cross-linked and noncleaved mutant NCKX2 protein is shifted downward to the same position occupied by the cleaved mutant NCKX2 protein without intramolecular cross-linking. D575C is located in helix H9, and the intramolecular cross-link between S185C or E188C in H2 and D575C in H9 would appear to have a slightly different shape (as judged by mobility on SDS−PAGE) when compared with the intramolecular cross-link generated between S185C or E188C and cysteine residues inserted into H8. Western blots such as the one illustrated in Figure 3A were scanned, and densitometry was used to quantify the degree of intramolecular cross-linking. In most cases, the two middle bands were not sufficiently resolved for unambiguous identification. Since the lowest band is likely to represent cross-linking of the cleaved NCKX2 mutant protein located in the plasma

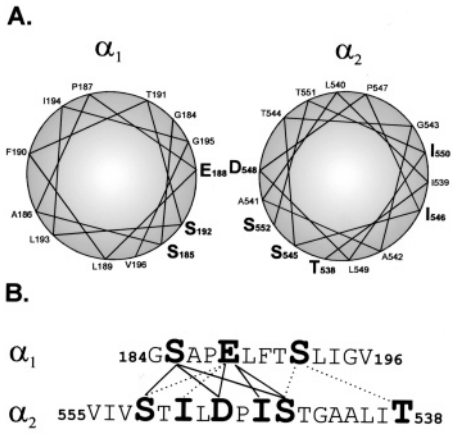

FIGURE 4: Summary of disulfide mapping between residues in helix H2 and residues in helix H8. (A) Helical wheel projections show the localization of the residues of helices H2 and H8 to hydrophilic (facing each other) and hydrophobic (facing away) surfaces, respectively. Residues in bold type were replaced with cysteine and used for disulfide mapping. (B) Summary of the disulfide mapping experiments concerning residues in helices H2 and H8 as illustrated in Figures 3, 5, and 6. Solid lines represent strong cross-links, while dotted lines represent weaker cross-links.

membrane (see below), we determined the percentage this band contributed to the total amount of mutant NCKX2 protein present. A significant amount of cross-linked and cleaved NCKX2 protein was observed for all eight mutants tested with the lowest cross-linking efficiency observed for the E188C/S552C NCKX2 mutant (Figure 3B). No significant differences in the cross-linking patterns were observed for the double cysteine insertion mutants illustrated in Figure 3 whether the medium contained predominantly Na^+ or whether the medium contained predominantly Ca^{2+} and K^+ (data not illustrated).

We analyzed a large number of double cysteine insertions into the Cys-less NCKX2 background outside of the two α repeats, and no shift in mobility was observed after copper−phenanthroline treatment in the large majority of these double cysteine insertion mutants. This suggests that, as expected, most pairs of inserted cysteine residues are not in sufficient proximity to form a disulfide bond. For example, we made a series of double cysteine insertions containing S266C, a residue located in the very short H4−H5 linker. S266C was paired up with each of five different residues thought to be located at the membrane−extracellular interface of H7 (A521), H8 (I534), H9 (L585), H10 (L603), and H11 (L650C), but none of the resulting five double cysteine insertion mutants exhibited any shift upon copper−phenanthroline treatment for up to 1 h at room temperature (not illustrated).

α-*Helical Structure of Helices H2 and H8?* In a helical wheel projection of helix H8, S552 and S545 are separated by two full turns, yet each of these two residues appears to be in the proximity of S185 (Figure 4). Figure 4 summarizes the results obtained in the experiments illustrated in Figure 3. Evidently, residues across two full turns of a putative α helix could form disulfide bonds. As a negative control to test the α-helical structure of H8, we examined residues I546 and I550, both of which are located on the hydrophobic surface of α2 repeat helix H8, away from the hydrophilic surface that contains D548, S545, and S552. The E188C/I546C and E188C/I550C NCKX2 mutants were made to

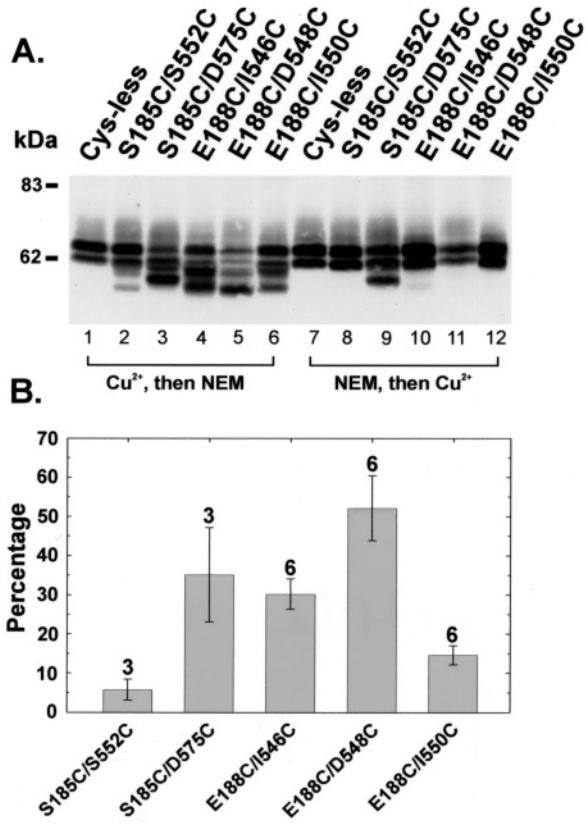

FIGURE 5: Formation of disulfide bonds between E188C and I546C or I550C. (A) The Cys-less NCKX2 protein and the indicated double cysteine insertion mutants in the Cys-less background were expressed in HEK293 cells and analyzed by SDS−PAGE when copper−phenanthroline treatment preceded incubation with NEM (lanes 1−6) or when the copper−phenanthroline and NEM treatments were reversed (lanes 7−12) as described in the text and in Experimental Procedures. Protein samples (20 μg of protein/lane) were separated by SDS−PAGE, and the Myc-tagged NCKX2 mutants were visualized with the monoclonal Myc antibody. Shifts in mobility compared with the Cys-less NCKX2 indicate intramolecular disulfide bond formation. Some smeared immunoreactivity was observed above the NCKX2 bands, and this was more pronounced in samples treated with NEM as is the case here. (B) Western blots of experiments such as the one illustrated in panel A were scanned and analyzed with the use of SigmaGel 1.0. The area representing the lowest band was expressed as the percentage of the total NCKX2 protein present (total area representing all bands). Average values (±standard error of the mean) are shown for the various NCKX2 mutants with the number of independent experiments indicated at the top of the bars.

examine the proximity of E188 to I546 and I550, both of which should be pointed away if H8 adopts an α-helical structure. Both E188C/I546C and E188C/I550C NCKX2 mutants were analyzed in HEK293 cells rather than High Five cells as no protein expression of these two mutants was observed in the latter. All samples were treated with copper−phenanthroline; the reaction was stopped by addition of excess EDTA, and subsequent treatment with NEM was used to alkylate all remaining free sufhydryl groups prior to addition of the lysis buffer (see Experimental Procedures). Control samples were only treated with NEM prior to addition of the lysis buffer. Strong disulfide bond formation was observed when incubation with copper−phenanthroline preceded NEM treatment in intact cells (Figure 5A, lanes 1−6). The four-band pattern observed for both E188C/I546C and E188C/I550C mutant NCKX2 proteins clearly indicates the presence of disulfide bonds in both cleaved and non-

cleaved populations of these two NCKX2 mutants (Figure 5A, lanes 4 and 6). For comparison, the S185C/S552C, S185C/D548C, and E188C/D575C double mutants were also analyzed in HEK cells with very similar results as obtained in High Five cells, although cross-linking of the S185C/S552C mutant NCKX2 (lane 2) was somewhat less efficient in HEK293 cells (compare Figures 3B and 5B). Note that this was one of the very few blots in which a four-band pattern was resolved for the S185C/D575C mutant NCKX2. When the order of copper−phenanthroline and NEM treatments was reversed, no disulfide cross-links were observed except for the S185C/D575C mutant NCKX2 (Figure 5A, lanes 7−12). This illustrates the efficacy of the NEM treatment in alkylating the inserted cysteine residues and suggests that no disulfide bonds had formed in the intact cells prior to addition of copper−phenanthroline except for the S185C/D575C mutant NCKX2 (Figure 5A, lane 9). To date, this represents the only double cysteine insertion mutant in which a disulfide cross-link had formed in situ, although it is unclear why this was not observed in the High Five cell system. The average cross-linking levels observed in three to six experiments are shown in Figure 5B.

Antiparallel Orientation of Helices H2 and H8. Helices H2 and H8 within the α1 and α2 repeats are thought to be in an antiparallel orientation (*20*) with key hydroxyl-containing residues being placed at various positions of the hydrophilic surface of both helices (*22, 26*) (Figure 4). We examined the ability of S192C in helix H2 to form disulfide bonds with each of three differently placed hydroxyl-containing residues on the hydrophilic face of helix H8 (T538, S545, and S552) (Figure 1). Consistent with the antiparallel orientation, S192C formed disulfide cross-links with T538C and S545C, but not with S552C (Figure 6, lanes 2−4). Although the experiment illustrated in Figure 6A included a 10 min incubation with copper−phenanthroline at room temperature, in most experiments longer incubation times of 45−60 min were required to obtain clear evidence for intramolecular cross-linking of the double cysteine insertion mutants that included S192C. The average cross-linking levels observed in five experiments are shown in Figure 6B.

Proximity of Residue D258 to Residues in Helices H8 and H2. Four acidic residues, important for NCKX2 function (*22, 23, 26*), are thought to be located in the horizontal midplane of the membrane (Figure 1). Data illustrated in Figure 3 indicate that E188 is in the proximity of both D548 and D575. We examined the proximity of D258 to various residues in helices H2 and H8 as substitution of D258 could cause shifts in both Ca^{2+} and K^+ concentration dependencies of reverse Na^+/Ca^{2+}-K^+ exchange (*22*). However, no formation of disulfide bonds between D258C and cysteine replacements of the other acidic residues located in either helix H2 (E188), H8 (D548), or H9 (D575) was observed (Figure 6A, lanes 10−12) even when long incubation times of 60 min were used.

Cross-Linking of the Double Cysteine Insertion Mutants Present in the Plasma Membrane. The results illustrated in Figure 2 show that, with the exception of the D258C/D575C NCKX2 mutant, signal peptide cleavage was not very different in the double cysteine insertion mutants which suggests that plasma membrane targeting was not affected in all but one of those mutants. To ensure that the subpopulation of mutant NCKX2 protein in the plasma membrane formed the intramolecular cross-links observed here, surface biotinylation (EZ-Link Sulfo-NHS-LC-Biotin) was combined with cross-linking (with copper−phenanthroline) as illustrated in Figure 7. As a negative control (lane 1), we used the Δ75N-NCKX2 deletion mutant which lacks the first 75 N-terminal residues containing the signal peptide and is not targeted to the plasma membrane (*19*). The Cys-less NCKX2 (lane 2) was used as a positive control for plasma membrane delivery since this mutant NCKX2 exhibits ∼50% of wild-type NCKX2 function but cannot undergo intramolecular disulfide bond formation (*24*). Cells expressing the mutant NCKX2 proteins were surface biotinylated, and the double cysteine insertion mutants were also treated with copper−phenanthroline and NEM (as described in Experimental Procedures). The mutant NCKX2 proteins were purified by immunoprecipitation with the monoclonal Myc antibody, separated on SDS−PAGE, and probed with avidin−HRP (Figure 7A, colored green). No band was observed for the truncated Δ75N-NCKX2 construct since the signal peptide is required for plasma membrane targeting. Strong surface biotinylation was observed for the Cys-less NCKX2 (lane 2) and all six double cysteine mutants (lanes 3−8), demon-

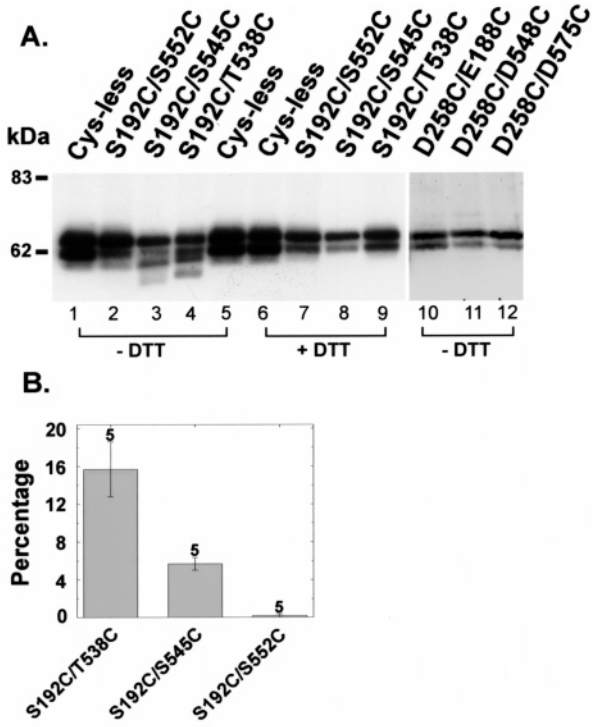

FIGURE 6: Antiparallel orientation of putative α helices H2 and H8. (A) The indicated double cysteine insertion mutant NCKX2 proteins were expressed in High Five cells and treated for 10 min with copper−phenanthroline as described in Experimental Procedures. Protein samples (20 μg of protein/lane) were separated by SDS−PAGE under nonreducing conditions or after addition of 1 mM DTT as indicated. The Myc-tagged NCKX2 mutants were visualized with the monoclonal Myc antibody. Shifts in mobility compared to the Cys-less NCKX2 indicate intramolecular disulfide bond formation. (B) Western blots of experiments such as the one illustrated in panel A were scanned and analyzed with the use of SigmaGel 1.0. The area representing the lowest band was expressed as the percentage of the total NCKX2 protein present (total area representing all bands). Average values (±standard error of the mean) are shown for the various NCKX2 mutants with the number of independent experiments indicated at the top of the bars.

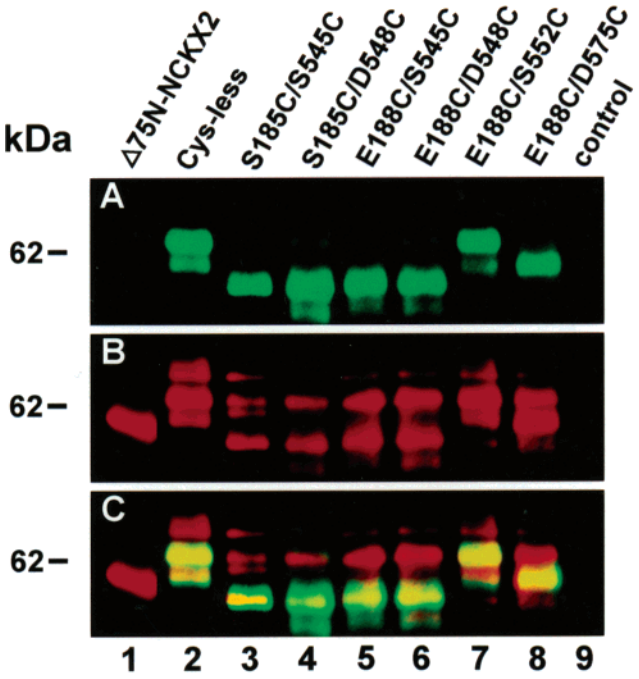

FIGURE 7: Surface biotinylation of double cysteine insertion NCKX2 mutants. Cys-less NCKX2, Δ75-NCKX2, and the indicated double cysteine insertion NCKX2 mutants in the Cys-less background were expressed in High Five cells. The Δ75-NCKX2 NCKX2 mutant is defined in the text and has been described previously (*17*). Control represents mock-transfected cells. Copper−phenanthroline and NEM treatment and surface biotinylation (with EZ-Link Sulfo-NHS-LC-Biotin) were carried out as described in Experimental Procedures. Protein was extracted in lysis buffer and, when indicated, immunoprecipitated with the monoclonal Myc antibody. Negative images of the blots were colored and merged with the use of Adobe Photoshop CS. (A) Avidin−HRP blot of biotinylated and immunopurified samples: lanes 1 and 2, no further treatment; and lanes 3−9, following biotinylation, treated with copper−phenanthroline and NEM. (B) Same blot as in panel A but stripped and reprobed with the polyclonal Myc antibody. (C) Merged image of panels A and B. Note that in this experiment the Cys-less NCKX2 exhibited an additional lower band that gives rise to a three-band pattern; this represents additional cleavage at the N-terminus, as described in the text.

strating that all were correctly targeted to the plasma membrane. Moreover, the double cysteine mutant NCKX2 proteins present in the plasma membrane ran at a lower MW than the Cys-less NCKX2, indicating that these mutant NCKX2 proteins had undergone complete intramolecular cross-linking. The only exception was the E188C/S552C NCKX2 mutant (lane 7) for which a considerable amount of cleaved protein without an intramolecular cross-link was present in the plasma membrane, consistent with the low cross-linking efficiency observed for this mutant in Figure 3. Next, the blot was stripped and reprobed with the polyclonal Myc antibody (Figure 7B, colored red). The truncated Δ75N-NCKX2 construct (lane 1) exhibited a single band at a lower MW compared with the band(s) observed for the Cys-less NCKKX2 (lane 2), consistent with the absence of the signal peptide through truncation of the first 75 residues (signal peptide cleavage of NCKX2 is predicted to occur at residue 58). In the High Five cell expression system, the lower band of NCKX2 was sometimes (as observed here) accompanied a "shadow" band with an even slightly lower MW, giving rise to a three-band pattern (both lower bands were present in the plasma membrane as judged by surface biotinylation, panel A). The lowest-MW band represents further N-terminal cleavage of NCKX2 beyond residue 62 as a Flag tag inserted at position 62 was no longer present in the Flag-tagged NCKX2 protein represented by this band (data not illustrated; the Flag-tagged NCKX2 constructs were described in ref *19*). Merging panels A and B demonstrates that only the cleaved band(s) of the Cys-less NCKX2 (lane 2) and the six double cysteine insertion mutants (lanes 3−8) were located in the plasma membrane. It also illustrates (consistent with the results shown in Figure 3) that the noncleaved double cysteine NCKX2 mutant protein not present in the plasma membrane also underwent intramolecular cross-linking. Results similar to those shown in Figure 7 were obtained in at least three other experiments for each of the eight double cysteine insertion mutants illustrated in Figure 3; similar results were also obtained with the double cysteine insertion mutants expressed in HEK293 cells (i.e., those illustrated in Figure 5) (data not shown).

DISCUSSION

Ion binding sites or selectivity filters of ion transporters and channels are typically comprised of residues located on several distinct membrane-spanning or membrane-penetrating segments that can be far apart in the linear protein sequence. In previous studies, we identified several residues within the α1 and α2 repeats of the NCKX2 protein that were important for maximal transport function (*26*), and/or showed altered K^+ and Ca^{2+} concentration dependencies upon substitution (*22*, *23*). Here, we used site-directed disulfide mapping to report on the spatial arrangement of these α repeats. The major novel finding in this study is that a set of key residues on membrane-spanning helices H2, H8, and H9 (Figure 1), suggested to line the cation binding pocket in NCKX2 (i.e., S185, E188, S545, D548, S552, and D575) (*22*, *23*), are in proximity in the native NCKX2 structure, although they are located in different membrane-spanning helices separated by ∼350 residues.

Three features stand out:

(1) The high incidence of disulfide bond formation observed for the residues studied here and thought to be located well within membrane-spanning helices is in sharp contrast with the low incidence of disulfide bond formation we observed when trying to map the proximity of the ends of the various membrane-spanning helices of NCKX2[2] or NCX1 (*27*).

(2) The disulfide cross-links observed in Figure 3 encompass a significant volume as two residues on helix H2 (S185 and E188) could each form cross-links with three different residues on helix H8 that are separated by close to two full turns of an α helix, suggesting an area of enhanced flexibility and movement. Helix movement is corroborated by the observation that E188C on helix H2 also formed cross-links with I546C and I550C (Figure 5), two residues thought to be on a hydrophobic surface of helix H8 facing away (Figure 4). Despite the flexibility suggested by the ability of different residues in the central portions of helices H2 and H8 to form disulfide cross-links, significant steric constraints exist as well for these residues as a mere lengthening of the side

[2] T. G. Kinjo, K.-J. Kang, R. T. Szerencsei, and P. P. M. Schnetkamp, manuscript in preparation.

chain by one methylene group caused a significant loss of NCKX2 function in four cases: the S185T, S545T, and S552T NCKX2 mutants (*22*) and the D575E NCKX2 mutant (*23*).

(3) In addition to residues in helix H8, S185C and E188C could each also form fast intramolecular disulfide cross-links with D575C on helix H9 (Figures 4−6), consistent with the crucial role of D575 in binding of K^+ to the NCKX2 cation binding pocket (*23*).

Two previous studies used a very similar strategy to map the proximity of residues involved in substrate binding within transmembrane helices of the P-glycoprotein and SERCA Ca^{2+} pump, respectively. For the P-glycoprotein, the frequency of cross-links was much lower than that observed here for NCKX2 (*28*). The SERCA Ca^{2+} pump was found to have a network of cross-links all along the length of membrane helices 4 and 6, but no cross-links were reported that would span two turns of the helix (*29*). In the latter study, the SERCA Ca^{2+} pump was "frozen" in the E_2 state which prevented cycling of the pump during the incubation with copper−phenanthroline. Unfortunately, it is not possible to freeze the NCKX protein in either an inward-facing or outward-facing conformation for the duration of the cross-link experiment. The cation binding sites of NCKX are thought to alternate from an outward-facing conformation to an inward-facing conformation (consecutive or "ping-pong" mechanism) during the cation transport cycle (*1*, *11*). We propose that the large number of cross-links observed here reflects relative movement of helices H2 and H8 with respect to each other during the conformational transition from inward- to outward-facing.

Do the Double Cysteine Mutant NCKX2 Proteins Represent the Wild-Type NCKX2 Structure? Since we examined residues that are critical for NCKX2 transport function, the double cysteine insertion mutants were nonfunctional and could conceivably represent misfolded proteins. We believe that the double cysteine mutants used here represent the wild-type NCKX2 structure and have no major folding deficiencies in view of the fact that they do not display the trafficking defects normally associated with folding deficiencies of plasma membrane proteins (*30*), for example, plasma membrane ion channel proteins such as the ΔF508 CFTR mutant (*31*) or several mutant hERG channels associated with long QT syndrome (*32*). (1) When analyzed on SDS−PAGE, all the double cysteine insertion mutants used in this study displayed the characteristic two-band pattern (Figures 2 and 3) which we previously showed to be caused by signal peptide cleavage associated with plasma membrane targeting (*19*). (2) Surface biotinylation was readily observed for all the double cysteine insertion mutants, and the subpopulation of biotinylated NCKX2 molecules found in the plasma membrane had undergone near-complete intramolecular cross-linking for most of double cysteine insertion NCKX2 mutants studied here (Figure 7).

Structure of Hydrophobic Segments H2 and H8. Within our current model of NCKX2 topology, H2 and H8 both form membrane-spanning α helices and would appear to have a well-defined orientation and demarcation of the membrane−aqueous medium interface (*20*). (1) A pair of aspartate residues appears to delineate the cytoplasmic N-terminal end of H2, while the extracellular C-terminal end contains two residues shown to be accessible to the extracellularly applied and impermeant sulfhydryl-modifying reagent MTSET. (2) The N-terminal end of H8 contains two adjacent acidic residues, while the cytoplasmic C-terminal end appears to be defined by a pair of basic residues. The resulting antiparallel orientation of H2 and H8 is consistent with the observation here that S192C could form disulfide cross-links with T538C and S545C, but not with S552C (Figure 6), but the reaction time was considerably slower than that for observed cross-links that involved S185C, S545C, or S552C. The S192 residue is well-conserved in NCKX proteins representing different isoforms or different species and would appear to be in a very similar position when compared with S185, S545, and S552. However, the slower reaction time for disulfide bond formation appears to correlate with the observation that S192 is not particularly critical for NCKX2 function as substitution with either alanine or cysteine had little effect (*26*).

The many cross-links that were observed between E188C on H2 and residues S545C, D548C, and S552C on H8 that span close to two full turns of an α helix, or between E188C and residues I546C and I550C that face away from the hydrophilic surface of H8 (summarized in Figure 4), imply an area of high flexibility. A recent survey of the placement of proline residues in membrane-spanning helices of proteins with known structure suggests the presence of structural elements in H2 and H8 of NCKX2 that would impart increased flexibility (*32*). This survey showed that a proline residue is often encountered in a central position in membrane-spanning helices, introducing a region of distortion and increased flexibility due to steric hindrance and loss of hydrogen bonds, especially if a glycine is present at position −3 or −4. Hinge motions are facilitated by a kink at the glycine position and a swivel of the C-terminal segment with respect to the N-terminal segment (*33*). The central portions of helices H2 and H8 of NCKX2 conform to this pattern with GGSAPEL (H2) and GTSPD (H8) sequences. Simple modeling of two interlocked and kinked α helices suggests that a corkscrew movement by one residue or ∼2 Å of H8 with respect to H2 can allow all the residues shown here to form disulfide cross-links within ∼3 Å of each other. This movement of helices H2 and H8 could reflect the conformational change when the cation binding pocket moves from an outward-facing conformation to an inward-facing conformation (consecutive or ping-pong mechanism) during the cation transport cycle. Movement during the NCKX transport cycle may bring S185 or E188 into the proximity of S552, D548, and S545 at different points in the transport cycle. Further experiments will be designed to try to freeze conformational states of NCKX and also to map the proximity of other residues on H2, H8, and H9.

REFERENCES

1. Schnetkamp, P. P. M. (2004) The SLC24 Na^+/Ca^{2+}-K^+ exchanger family: Vision and beyond, *Eur. J. Physiol. 447*, 683−688.
2. Cai, X., and Lytton, J. (2004) Molecular cloning of a sixth member of the K^+-dependent Na^+/Ca^{2+} exchanger gene family, NCKX6, *J. Biol. Chem. 279*, 5867−5876.
3. Szerencsei, R. T., Tucker, J. E., Cooper, C. B., Winkfein, R. J., Farrell, P. J., Iatrou, K., and Schnetkamp, P. P. M. (2000) Minimal Domain Requirement for Cation Transport by the Potassium-dependent Na/Ca-K Exchanger: Comparison with an NCKX Paralog from *Caenorhabditis elegans*, *J. Biol. Chem. 275*, 669−676.

4. Haug-Collet, K., Pearson, B., Park, S., Webel, R., Szerencsei, R. T., Winkfein, R. J., Schnetkamp, P. P. M., and Colley, N. J. (1999) Cloning and Characterization of a Potassium-Dependent Sodium/Calcium Exchanger in *Drosophila*, *J. Cell Biol. 147*, 659−669.
5. Su, Y. H., and Vacquier, V. D. (2002) A flagellar K^+-dependent Na^+/Ca^{2+} exchanger keeps Ca^{2+} low in sea urchin spermatozoa, *Proc. Natl. Acad. Sci. U.S.A. 99*, 6743−6748.
6. Winkfein, R. J., Pearson, B., Ward, R., Szerencsei, R. T., Colley, N. J., and Schnetkamp, P. P. M. (2004) Molecular characterization, functional expression and tissue distribution of a second NCKX Na^+/Ca^{2+}-K^+ exchanger from *Drosophila*, *Cell Calcium 36*, 147−155.
7. Palty, R., Ohana, E., Hershfinkel, M., Volokita, M., Elgazar, V., Beharier, O., Silverman, W. F., Argaman, M., and Sekler, I. (2004) Lithium−Calcium Exchange Is Mediated by a Distinct Potassium-independent Sodium−Calcium Exchanger, *J. Biol. Chem. 279*, 25234−25240.
8. Schnetkamp, P. P. M., Basu, D. K., and Szerencsei, R. T. (1989) Na-Ca exchange in the outer segments of bovine rod photoreceptors requires and transports potassium, *Am. J. Physiol. 257*, C153−C157.
9. Szerencsei, R. T., Prinsen, C. F. M., and Schnetkamp, P. P. M. (2001) The Stoichiometry of the Retinal Cone Na/Ca-K Exchanger Heterologously Expressed in Insect Cells: Comparison with the Bovine Heart Na/Ca Exchanger, *Biochemistry 40*, 6009−6015.
10. Dong, H., Light, P. E., French, R. J., and Lytton, J. (2001) Electrophysiological characterization and ionic stoichiometry of the rat brain K^+-dependent Na^+/Ca^{2+} exchanger, NCKX2, *J. Biol. Chem. 276*, 25919−25928.
11. Schnetkamp, P. P. M. (1989) Na-Ca or Na-Ca-K exchange in the outer segments of vertebrate rod photoreceptors, *Prog. Biophys. Mol. Biol. 54*, 1−29.
12. Lagnado, L., and McNaughton, P. A. (1990) Electrogenic Properties of the Na:Ca Exchange, *J. Membr. Biol. 113*, 177−191.
13. Schnetkamp, P. P. M. (1995) Calcium homeostasis in vertebrate retinal rod outer segments, *Cell Calcium 18*, 322−330.
14. Schwarzer, A., Schauf, H., and Bauer, P. J. (2000) Binding of the cGMP-gated channel to the Na/Ca-K exchanger in rod photoreceptors, *J. Biol. Chem. 275*, 13448−13454.
15. Poetsch, A., Molday, L. L., and Molday, R. S. (2001) The cGMP-gated channel and related glutamic acid-rich proteins interact with peripherin-2 at the rim region of rod photoreceptor disc membranes, *J. Biol. Chem. 276*, 48009−48016.
16. Kang, K.-J., Bauer, P. J., Kinjo, T. G., Szerencsei, R. T., Bonigk, W., Winkfein, R. J., and Schnetkamp, P. P. M. (2003) Assembly of Retinal Rod or Cone Na^+/Ca^{2+}-K^+ exchangers oligomers with cGMP-gated channel subunits as probed with heterologously expressed cDNAs, *Biochemistry 42*, 4593−4600.
17. Picones, A., and Korenbrot, J. I. (1995) Permeability and interaction of Ca^{2+} with cGMP-gated ion channels differ in retinal rod and cone photoreceptors, *Biophys. J. 69*, 120−127.
18. Dzeja, C., Hagen, V., Kaupp, U. B., and Frings, S. (1999) Ca^{2+} permeation in cyclic nucleotide-gated channels, *EMBO J. 18*, 131−144.
19. Kang, K.-J., and Schnetkamp, P. P. M. (2003) Signal sequence cleavage and plasma membrane targeting of the rod NCKX1 and cone NCKX2 Na^+/Ca^{2+}-K^+ exchangers, *Biochemistry 42*, 9438−9445.
20. Kinjo, T. G., Szerencsei, R. T., Winkfein, R. J., Kang, K.-J., and Schnetkamp, P. P. M. (2003) Topology of the retinal cone NCKX2 Na/Ca-K exchanger, *Biochemistry 42*, 2485−2491.
21. Cai, X., Zhang, K., and Lytton, J. (2002) A novel topology and redox regulation of the rat brain K^+-dependent Na^+/Ca^{2+} exchanger, NCKX2, *J. Biol. Chem. 277*, 48923−48930.
22. Kang, K.-J., Kinjo, T. G., Szerencsei, R. T., and Schnetkamp, P. P. M. (2005) Residues contributing to the Ca^{2+} and K^+ binding pocket of the NCKX2 Na^+/Ca^{2+}-K^+ exchanger, *J. Biol. Chem. 280*, 6823−6833.
23. Kang, K.-J., Shibukawa, Y., Szerencsei, R. T., and Schnetkamp, P. P. M. (2005) Substitution of a single residue, Asp^{575}, renders the NCKX2 K^+-dependent Na^+/Ca^{2+} exchanger independent of K^+, *J. Biol. Chem. 280*, 6834−6839.
24. Kinjo, T. G., Szerencsei, R. T., Winkfein, R. J., and Schnetkamp, P. P. M. (2004) Role of cysteine residues in the NCKX2 Na^+/Ca^{2+}-K^+ exchanger: Generation of a functional cysteine-free exchanger, *Biochemistry 43*, 7940−7947.
25. Prinsen, C. F. M., Szerencsei, R. T., and Schnetkamp, P. P. M. (2000) Molecular cloning and functional expression of the potassium-dependent sodium-calcium exchanger from human and chicken retinal cone photoreceptors, *J. Neurosci. 20*, 1424−1434.
26. Winkfein, R. J., Szerencsei, R. T., Kinjo, T. G., Kang, K.-J., Perizzolo, M., Eisner, L., and Schnetkamp, P. P. M. (2003) Scanning mutagenesis of the α repeats and of the transmembrane acidic residues of the human retinal cone Na/Ca-K exchanger, *Biochemistry 42*, 543−552.
27. Qiu, Z., Nicoll, D. A., and Philipson, K. D. (2001) Helix packing of functionally important regions of the cardiac Na^+-Ca^{2+} exchanger, *J. Biol. Chem. 276*, 194−199.
28. Loo, T. W., Bartlett, M. C., and Clarke, D. M. (2004) Val^{133} and Cys^{137} in Transmembrane Segment 2 Are Close to Arg^{935} and Gly^{939} in Transmembrane Segment 11 of Human P-glycoprotein, *J. Biol. Chem. 279*, 18232−18238.
29. Rice, W. J., Green, N. M., and MacLennan, D. H. (1997) Site-directed disulfide mapping of helicers M4 and M6 in the Ca^{2+} binding domain of SERCA1a, the Ca^{2+}ATPase of fast twitch skeletal muscle sarcoplasmic reticulum, *J. Biol. Chem. 272*, 31412−31419.
30. Ellgaard, L., and Helenius, A. (2003) Quality control in the endoplasmic reticulum, *Nat. Rev. Mol. Cell Biol. 4*, 181−191.
31. Sharma, M., Pampinella, F., Nemes, C., Benharouga, M., So, J., Du, K., Bache, K. G., Papsin, B., Zerangue, N., Stenmark, H., and Lukacs, G. L. (2004) Misfolding diverts CFTR from recycling to degradation: Quality control at early endosomes, *J. Cell Biol. 164*, 923−933.
32. Thomas, D., Kiehn, J., Katus, H. A., and Karle, C. A. (2003) Defective protein trafficking in hERG-associated hereditary long QT syndrome (LQT2): Molecular mechanisms and restoration of intracellular protein processing, *Cardiovasc. Res. 60*, 235−241.
33. Cordes, F. S., Bright, J. N., and Sansom, M. S. (2002) Proline-induced distortions of transmembrane helices, *J. Mol. Biol. 323*, 951−960.

BI0502442